Novel tethered particle motion analysis of CI protein-mediated DNA looping in the regulation of bacteriophage lambda

2006 J. Phys.: Condens. Matter 18 S225

(http://iopscience.iop.org/0953-8984/18/14/S07)

INSTITUTE OF PHYSICS PUBLISHING JOURNAL OF PHYSICS: CONDENSED MATTER

J. Phys.: Condens. Matter **18** (2006) S225–S234 doi:10.1088/0953-8984/18/14/S07

Novel tethered particle motion analysis of CI protein-mediated DNA looping in the regulation of bacteriophage lambda

C Zurla[1,4], A Franzini[1], G Galli[1], D D Dunlap[2,5], D E A Lewis[3], S Adhya[3] and L Finzi[1,4,6]

[1] Department of Biology, University of Milan, Via Celoria 26, 20133 Milan, Italy
[2] ALEMBIC, San Raffaele Scientific Institute, Via Olgettina 58, 20132 Milan, Italy
[3] Laboratory of Molecular Biology, National Cancer Institute, National Institutes of Health, Bethesda, MD 20892-4264, USA

E-mail: lfinzi@emory.edu

Received 10 October 2005
Published 24 March 2006
Online at stacks.iop.org/JPhysCM/18/S225

Abstract

The tethered particle motion (TPM) technique has attracted great interest because of its simplicity and the wealth of information that it can provide on protein-induced conformational changes in nucleic acids. Here we present an approach to TPM methodology and analysis that increases the efficiency of data acquisition and facilitates interpretation of TPM assays. In particular, the statistical analysis that we propose allows fast data processing, minimal data selection and visual display of the distribution of molecular behaviour. The methodology proved useful in verifying CI protein-mediated DNA looping in bacteriophage λ and in differentiating between two different types of loops, stable and dynamic, whose relative occurrence seems to be a function of the distance between the operators as well as their relative angular orientation. Furthermore, the statistical analysis indicates that CI binding *per se* slightly shortens the DNA.

1. Introduction

The tethered particle motion (TPM) technique, or tethered particle microscopy as it has more recently been called, consists of observing through an optical microscope the Brownian motion of a small particle (bead) tethered to the glass surface of a microscope flow chamber by a single

[4] Present address: Department of Physics, Emory University, 400 Dowman Drive, N.E., Atlanta, GA 30322, USA.
[5] Present address: Department of Cell Biology, Emory University School of Medicine, 615 Michael Street, Atlanta, GA 30322, USA.
[6] Author to whom any correspondence should be addressed.

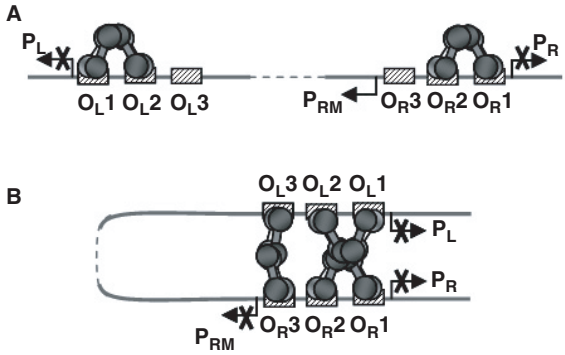

Figure 1. Model of CI regulation by long-range DNA looping proposed by Dodd and collaborators [7]. (A) CI dimers bound cooperatively at O_R1 and O_R2 repress transcription at P_R while the dimer at O_R2 also activates transcription from P_{RM}. The dimers bound cooperatively at O_L1 and O_L2 repress transcription at P_L. (B) Tetramers of CI bound at O_L and O_R interact forming an octameric complex and a 2.4 kbp DNA loop. This higher-order complex facilitates cooperative binding of another pair of CI dimers at O_L3 and O_R3, resulting in formation of another CI tetramer and repression of transcription from P_{RM}.

molecule of nucleic acid. The tether is invisible, but the range of Brownian motion of the bead depends on the length of its tether and can thus be used to infer the length of nucleic acid tethers. Furthermore, temporal changes in the Brownian motion can be used to monitor changes in tether length over time [1, 2]. Here we present a novel approach to TPM methodology and analysis which we tested on the bacteriophage λ system, a model for DNA-based genetic switching of transcription.

In eukaryotes, activation and repression of promoter activity are often achieved by means of proteins bound to enhancer or silencer elements located several kilobase pairs (kbp) away from the promoter. In prokaryotes, most regulatory protein-binding sites are located within 300 bp of the promoter, even if some gene regulators are known to work over larger distances. Recently, it has been discovered that the well studied CI protein of bacteriophage λ interacts over large distances, up to 3.6 kbp, and such interaction is essential for the stability of λ in the prophage state, present in the bacterial chromosome [3]. After the infection of *Escherichia coli* bacteria by λ, the phage can follow either one of two different pathways: (1) lysogeny, when the virus integrates its DNA into the host bacterial DNA and duplicates during bacterial cell division or (2) lysis, when the virus uses the bacterial molecular machinery to produce many viral copies after lysing the host cell. Once the virus enters the lysogenic state it can be induced to switch to lytic growth through a process called prophage induction. However, lysogeny is extremely stable: recent data indicate that less than one in 10^7–10^8 lysogenic cells spontaneously lyse per generation [4]. Despite the extreme stability of the lysogen, prophage induction takes place with essentially 100% efficiency. Lysogeny is stably maintained in the absence of an inducing signal (e.g. UV irradiation), but the system is poised to efficiently change upon receiving the signal for the lytic pathway. In the prophage state, all the phage promoters, except the one that transcribes the CI gene, are turned off. By contrast, during lytic growth, most other phage genes are expressed [5]. The CI repressor protein has a key role in the λ genetic switch. CI is both an activator and a repressor of transcription and is required for the maintenance of the lysogenic state. During lysogeny, dimers of CI bind to specific sites within the O_L and O_R control regions, located about 2.4 kbp apart on the phage genome (figure 1). Each control region contains three operators, O_L1, O_L2, O_L3 and O_R1, O_R2, O_R3.

The cooperative binding of CI to O_R1 and O_R2 represses transcription from the P_R promoter. Similarly, the binding of CI to O_L1 and O_L2 represses transcription from the P_L promoter. By doing so, tetramers of CI inhibit the transcription of the phage's lytic genes from P_R and P_L and, simultaneously, activate the transcription of the CI gene from the promoter P_{RM} [6]. CI is also able to negatively regulate its own synthesis when present at high concentrations. This was explained by a model, proposed by Dodd and collaborators [7], suggesting that tetramers of CI bound to O_L1, O_L2 and O_R1, O_R2 interact to form an octamer and the intervening DNA sequence loops out. This higher-order DNA structure juxtaposes O_L3 and O_R3 so that a CI dimer bound at O_L3 can assist a CI dimer bound at O_R3, resulting in the repression of P_{RM}. This model of negative autoregulation would limit the concentration of CI in the lysogenic state and permit efficient switching to the lytic stage.

We performed single TPM measurements on λ DNA fragments containing both O_L and O_R regions in the hope of investigating the formation and dynamics of CI-mediated DNA looping. First we developed an experimental and analytical procedure for producing and selecting beads that are tethered by single, and not multiple, DNA molecules that are uniform in length. Secondly we used a calibration curve produced in the laboratory (manuscript submitted) that allows prediction of the DNA length expected for the unlooped and looped DNA conformations in a tethered state. Thirdly we analysed the ability of CI protein to loop DNA as a function of (1) distance between the O_L and O_R regions and (2) the involvement of the O_L region in looping.

2. Experimental and theoretical approach

2.1. Plasmids and DNA fragments for TPM

Lambda DNA (New England Biolabs GmbH, Frankfurt am Main, Germany) was used as a template for polymerase chain reaction (PCR) amplification with primers from Sigma Genosys (The Woodlands, TX, USA) to generate two DNA fragments, one containing the O_R region and one containing the O_L region. The O_L region was amplified using the following primers: phageEcoRI 5′-ttctgctttGAATTCtgcccttcttcagggcttaatttttaagagcgtcaccttcatgg-3′ and lambdaAvr/Bgl-B 5′-cgccgcCCTAGGttgcaaaaattAGATCTctcacctaccaaacaatgccccccctgcaaaaaataaattcatataaaaaacatacag-3′, where the capital letters represent engineered restriction sites. The O_R region was amplified using the following primers: lambdaBgl/Avr-T 5′-gtttggtaggtgagAGATCTaatttttgcaaCCTAGGcggcgttataagcatttaatgcattgatgccattaaataaagcacc-3′ and phagePstI 5′-cgccgagtaCTGCAGctgtcttggtttgcccaaagcgcattgcataatctttcaggg-3′. The overlapping PCR products were mixed and extended by PCR reaction in the presence of phageEcoRI and phagePstI primers. The resulting product is a DNA fragment containing the complete O_L and O_R regions with a distance of 300 bp between the centre of O_L3 and O_R3 operators. Such a fragment, named 'fragment 300', was inserted into plasmid pSA850 [8] between the *Eco*RI and *Pst*I restriction sites. The resulting plasmid was named pCZ300. Plasmid pCZ300 was then used as a template for PCR amplification of two different DNA fragments where the O_R and O_L regions are separated by 302 and 306 bp, respectively. The first fragment, 'fragment 302', was obtained by using primers phageins2 5′-caacgctaacAGATCTaaca tttttgcaaCCTAGGcggcgttataagcatttaatgcattgatgccattaaataaagcaccaacgcc-3′ (underlined bases represent those that were inserted) and phagePstI. The second fragment, 'fragment 306', was obtained by using phageins6 5′-caacgctaacAGATCTaacatgcatttttgcaaCCTAGGcggcgttataag catttaatgcattgatgccattaaataaagcaccaacgcc-3′ and phagePstI. Subsequently, plasmids pCZ302 and pCZ306 were obtained by digesting fragments 302 and 306 with *Bgl*II and *Pst*I and cloning them into the pCZ300, which was also digested with the same enzymes. Plasmid pCZ300 was

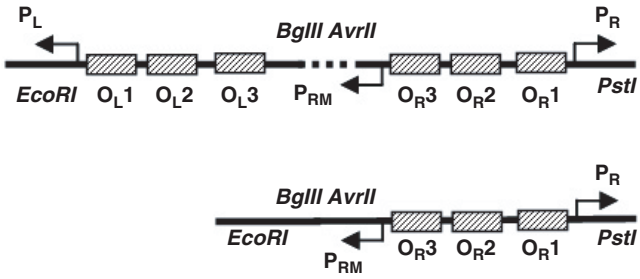

Figure 2. DNA fragments for TPM measurements. The 302, 306 and 1051 DNA fragments contain the complete O_L and O_R regions (the operators are represented as hatched boxes) separated by spacers of increasing lengths (dashed lines) inserted between the restriction sites *Bgl*II and *Avr*II. The delOL1-2-3 DNA fragment lacks the entire O_L region.

also used as a template to amplify a DNA fragment lacking the O_L operators using forward primer 5′-atcaccgcaGAATTCtatctgtatgttttttatatgaatttatttttgcaggggg-3′ and primer HinD3-6 reverse 5′-GTGCTGCAAGGCGATTAAGTTGGGTAACGCCAGGG-3′. The resulting product is the DNA fragment delOL1-2-3 that lacks the O_L region. Plasmid pCZdelOL1-2-3 was obtained by digesting 'fragment delOL1-2-3' with *Eco*RI and *Hind*III before cloning it into pSA850, which was digested with the same enzymes.

Plasmid pDLZ300 was obtained by cleaving pCZ300 with *Eco*RI and *Hind*III before cloning the smaller fragment containing the λ DNA it into plasmid pDL611 (obtained from pSA850 by the insertion of the T1T2 terminator between the *Kpn*I and *Eco*RI restriction sites). Finally, plasmid pDL1051 was obtained from plasmid pDLZ300 by inserting a 1100 bp fragment from bacteriophage λ DNA between *Bgl*II and *Avr*II restriction sites. This fragment from bacteriophage λ was amplified using primers phageEcoRI and lambdaAvrIII 5′-taacccgtcaCCTAGGttttcagacattagccctgcgggcaaaagatgaggccgg-3′. All the DNA fragments used in TPM (302, 306, 1051 and delOL1-2-3) were obtained by PCR in the presence of a biotin-labelled primer 5′-CGCAATTAATGTGAGTTAGCTCACTCATTAGGCACCCCAGGC-3′ and a digoxigenin-labelled primer 5′-GCATTGCTTATCAATTTGTTGCAACGAACAGGTC ACTATCAGTC-3′ (Oligos Etc., Inc., Wilsonville, OR, USA). The characteristics of the fragments described are summarized in figure 2.

2.2. *Preparation of the flow chamber and particle tracking*

The flow chambers for TPM measurements were similar to those described by Finzi and Dunlap [9]. A flow chamber was incubated over night at 4 °C with biotin-labelled bovine serum albumin (BSA) (40 μg ml^{-1}; Sigma-Aldrich, Inc., St Louis, MO, USA). After washing with 800 μl of buffer (10 mM Tris-HCl pH 7.4, 200 mM KCl, 5% dimethyl sulphoxide (DMSO), 0.1 mM EDTA, 0.2 mM dithiothreitol (DTT) and 0.1 mg ml^{-1}α-casein), the chamber was incubated for 2 h with streptavidin (50 μg ml^{-1}; Sigma-Aldrich). After washing the flow chamber with 800 μl of buffer, DNA in the pM range was introduced into the chamber and incubated for 1 h. This DNA, labelled at one end with biotin and at the other with digoxigenin was pre-incubated for 2 h with an excess of antidigoxigenin-coated beads (430 nm in diameter, Indicia Diagnostics, Oullins, France) in buffer lacking DTT and DMSO. Finally, the unbound DNA and unattached beads were flushed from the chamber with buffer.

Samples were observed through a differential interference contrast (DIC) microscope. The microscope (Leica DM LB) was equipped with a 100× oil-immersion objective, with a

numerical aperture of 1.4 (N-Plan). Images were obtained with a Jai CV-A60 camera, a CCD camera that outputs at a video rate of 25 frames s^{-1}; each field was exposed for 1/1000 s. The video signal was acquired later with a National Instruments IMAQ PCI-1409 frame grabber. The images were analysed using in-house software to determine the x and y coordinates of the bead versus time. The average over 4 s (100 points) of the coordinates x and y of the position of the bead establishes the coordinates x' and y' of the anchor point of the DNA on the glass. The mean square deviation allows the calculation of the distance of each point (position of the bead) from the tethering point and represents the amplitude of the motion of the bead $\sigma^2 = \langle (x - x')^2 + (y - y')^2 \rangle$. Control measurements, in the absence of CI, were recorded over 10 min. Measurements in the presence of CI were recorded over 20 min.

2.3. Bead selection

The data derived from each measurement, before and after protein addition, were analysed as follows. First σ was plotted versus time to visualize the amplitude of the bead motion and its changes during the time of observation. Secondly the displacement of the coordinates δx and δy of the centre of the bead from their average value was graphed as a function of time. In this way, we can exclude from the statistical analysis the beads that have an anisotropic motion that might be due to multiple tethers (5%) [2]. Thirdly the distribution of the x and y coordinates of each bead was plotted as a function of time in order to verify whether tracking was successful. In 10% of the cases there were discontinuities in the tracking of the bead position either due to loose particles moving across the image or to the rupture of the DNA tether. Finally, only those beads whose motion was tracked both before and after the addition of the protein were further analysed. The singly tethered beads were then analysed in two different ways as follows.

2.4. Manual data analysis

This analysis was based on the classification of time courses of sigma values by eye. Controls displayed traces with sigma characteristic of the unlooped conformation of the DNA molecule. After addition of protein, a new DNA conformation was often induced, and a lower average value was found to be stable or intermittent. Traces were divided into four groups after the addition of protein: (1) those whose sigma values did not change; (2) those that displayed a stable sigma reduced to the value expected for a looped DNA tether; (3) those that displayed step-like transitions between the sigma values in groups 1 and 2; and (4) those with noisy sigma values. The beads in the third group, showing transitions between the higher and the lower values of sigma, most likely switched between the unlooped and the looped conformation of the DNA tether. In the analysis of these events, only transitions lasting more that 20 s were counted, because transitions shorter than 20 s could be the result of random events. The beads in the fourth group, showing noisy traces, might have been tethered by a DNA molecule shorter than expected either due to shearing during preparation or partial adsorption of DNA on the glass. These beads often stuck to the surface of the microchamber during the time of observation.

Since this overall method of analysis may be subjected to the experimenter's error and bias, the following more objective analysis was developed.

2.5. Statistical analysis

This analysis extracts statistical information on the $\sigma(t)$ value of DNA conformations, along with the characteristic time of each conformation. For any given $\sigma(t)$ we evaluate

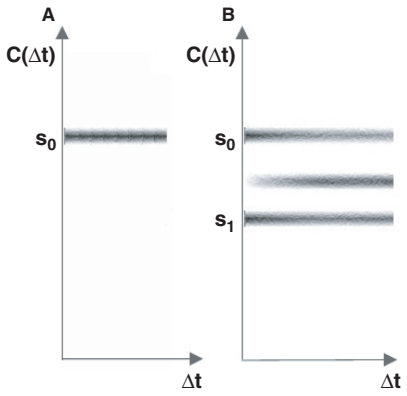

Figure 3. Ideal images of the probability density $P(\Delta t, C(\Delta t))$ (A) in the case where the bead shows an average sigma value around s_0 and (B) in the case where the bead shows transitions between two values, s_0 (unlooped) and s_1 (looped) corresponding to two distinct states.

$M(t, \Delta t)^2 = (\sigma(t) * \sigma(t + \Delta t))$. The two-point correlation function $C(\Delta t)$ is the root square of the average over t of $M(t, \Delta t)^2$. Plotting $C(\Delta t)$ as a function of Δt, we obtain an image representing the probability density, $P(\Delta t, C(\Delta t))$. In such image, the pixel grey-scale intensity is proportional to $P(\Delta t, C(\Delta t))$. When $\sigma(t)$ is nearly constant, $M(t, \Delta t)^2$ is essentially constant as a function of Δt and t and is affected only by white noise. Similarly $C(\Delta t)$ is constant over Δt, so the image $P(\Delta t, C(\Delta t))$ is, in this case, a horizontal band of uniform intensity at a height s_0 (figure 3(A)). The image $P(\Delta t, C(\Delta t))$ is more complex when $\sigma(t)$ shows transitions between two states having average $\sigma(t)$ values s_0 and s_1 and time constants τ_0 and τ_1, respectively. For time differences, Δt, shorter than τ_0 and τ_1, $\sigma(t)$ and $\sigma(t + \Delta t)$ are either equal to s_0 or to s_1. Thus, $C(\Delta t)$ is nearly always equal to either s_0 or s_1. Therefore, in this case, the image will display two horizontal bands, one centred around s_0 and the other centred around s_1. Alternatively, for a time difference Δt longer than τ_0 and τ_1, $\sigma(t)$ and $\sigma(t + \Delta t)$ have a probability of being equal to s_0 or s_1 proportional to τ_0 and τ_1, respectively. Therefore, $M(t, \Delta t)^2$ will have an average value approximately equal to $(s_0 * s_1)$, and $C(\Delta t)$ will be between s_0 and s_1.

In this case, the resulting image will show three bands: (1) the horizontal band at s_0 that will tend to disappear as Δt reaches τ_0, (2) the horizontal band at s_1 that will tend to disappear as Δt reaches τ_1 and (3) a horizontal band between the previous two bands that will gradually appear for the same values of Δt (figure 3(B)). The gradient in intensity of these bands is a measure of the lifetime of different states of the DNA tether.

$P(\Delta t, C(\Delta t))$ is evaluated over all traces obtained from any trackable bead.

s_0 and s_1 correspond to the unlooped and looped DNA conformations as confirmed by the calibration curve constructed in our laboratory (manuscript submitted).

3. Results and discussion

3.1. Effect of CI on DNA conformation

In order to study the effect of CI binding to DNA, we synthesized a set of DNA fragments containing the complete O_L and O_R regions at different distances and a fragment in which the O_L region was deleted (see figure 2).

Table 1. Percentage of beads counted in the unlooped, stably looped and transiently looped conformations, or showing non-specific sticking in the absence (−) and presence (+) of 100 nM CI using DNA fragments 302, delOL1-2-3, 306 and 1051.

	302		delOL1-2-3		306		1051	
CI 100 nM	−	+	−	+	−	+	−	+
Unlooped	91%	35%	100%	94%	87%	71%	85%	22%
Stably looped	4.5%	35%	0	0	0	13%	5.5%	19%
Dynamic looping	0	22.5%	0	0	0	5%	0	48%
Non-specific sticking	4.5%	6.5%	0	6%	13%	11%	9.5%	11%
Total number of beads analysed	39	31	63	47	47	38	55	54

3.2. CI-mediated DNA conformational changes: effect of distance and phase between the O_L and O_R regions and role of the O_L region

We analysed three DNA fragments where the two operators O_L and O_R are separated by 302, 306 and 1051 bp (figure 2). These DNA molecules are 1092, 1096 and 2211 bp long, respectively. TPM measurements performed using these DNA fragments were carried out first for 10 min, in the absence of protein, then for 20 min or more after addition of CI. We tracked the same beads before and after the addition of CI. We used two different concentrations of CI, 20 and 100 nM, at which some beads showed transitions between the expected $\sigma(t)$ for unlooped and looped DNA. In the control experiments, in the absence of CI, the large majority of beads showed a value of σ of about 210 nm for fragments 302 and 306, and 280 nm for fragment 1051 (figure 4(A)) as expected from our calibration curve (manuscript submitted). Vice versa, the expected value of $\sigma(t)$ for the looped conformation was about 175 nm in fragments 302 and 306 and about 210 nm in fragment 1051.

Table 1 summarizes the results obtained from manual analysis of the TPM measurements performed. A small percentage of beads tethered by fragments 302 and 1051 showed low values of $\sigma(t)$ in the controls, probably due to non-specific adsorption of DNA on the glass surface. After addition of the protein to fragments 302 and 1051, most of the DNA tethers showed either stable or dynamic looping.

DNA fragment 1051 seemed to be more prone to undergo dynamic (figures 4(C) and (D)) as opposed to stable looping (figure 4(B) and table 1), while the opposite was true for fragment 302. On the other hand, fragment 306, where O_L and O_R operators are out of phase, remained mostly unlooped (table 1). In support of our interpretation of these experiments, tethers lacking the O_L region did not show any CI-induced DNA looping.

3.3. Results of the statistical analysis

Since manual analysis is arduous and may be biased, we were interested in comparing the results reported in table 1 with those obtained using the statistical analysis described previously. The results of such analysis performed on DNA fragments 302, 306 and 1051 in the absence and presence of CI are illustrated in figure 5. The $P(\Delta t, C(\Delta t))$ images of the control experiments showed a marked horizontal band at the height expected for the unlooped conformation, in agreement with the data reported in table 1. The $P(\Delta t, C(\Delta t))$ images of the measurements conducted on fragments 302 and 306 in the presence of 20 nM CI still showed a strong band corresponding to unlooped tethers. However, the band was slightly shifted down with respect to the control, probably as a result of the partial occupation of the O_L and O_R operators that does not bring about DNA looping but results in local deformation, such as kinking, of the

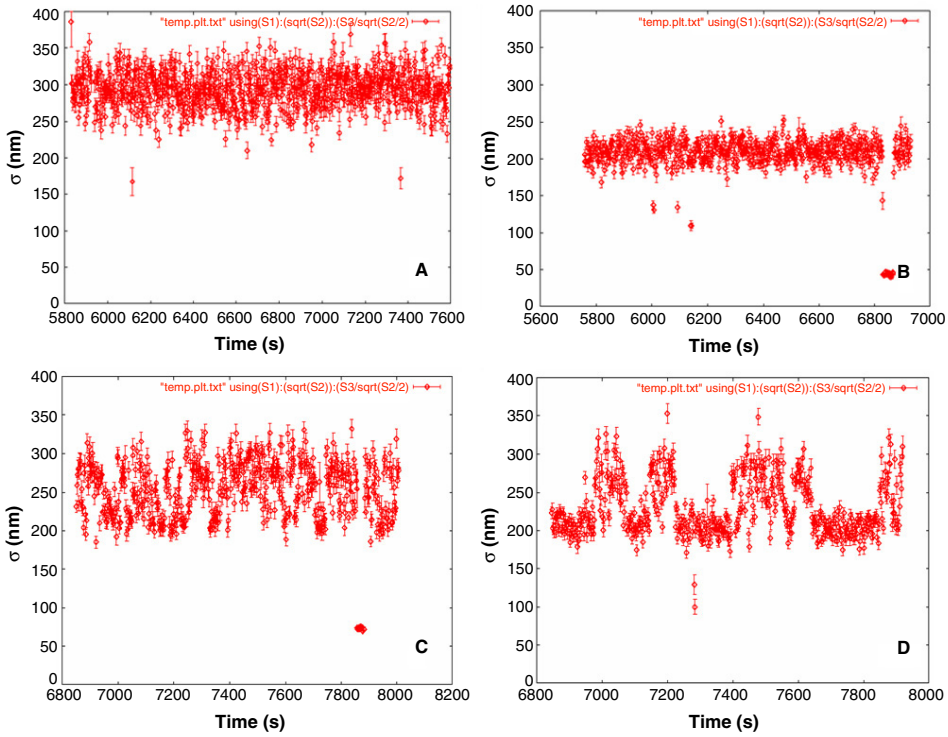

Figure 4. σ as a function of time for beads tethered by DNA fragment 1051: (A) $\sigma = 280$ nm in the control experiment; (B) stable loop formation at 210 nm in the presence of 100 nM CI; ((C) and (D)) two different DNA-tethered beads showing transitions between the unlooped and looped conformations.

(This figure is in colour only in the electronic version)

double helix. The lower protein concentration did not have any effect on the conformation of fragment 1051. In the presence of 100 nM CI, two bands are visible, one corresponding to the expected unlooped conformation and one whose height corresponded to the level expected for the looped state. In agreement with the results shown in table 1, the looped conformation was more probable than the unlooped one in the experiments using fragments 302 and 1051, while the opposite holds true for fragment 306. The additional weaker bands might be due to beads tethered by a DNA molecule shorter than expected either by preparation or because it was partially adsorbed on the surface of the glass, since no selection was made in this respect.

Figure 6 shows the results of the deletion of the O_L operators on CI-mediated DNA looping. In agreement with the data reported in table 1, looping was abrogated. Interestingly, this deletion also eliminated the shift of the unlooped band.

We conclude that statistical analysis was comparable to manual analysis and allows fast data processing and minimal data selection. Furthermore, this permits objective analysis of the data. Also, the statistical analysis proposed here better displays the distribution of molecular behaviours, and renders their classification easier than manual analysis. In particular, our methodology proved useful for verifying CI-mediated DNA looping and revealed two different types of looping, stable and dynamic, whose relative occurrence is a function of distance between the operators. Moreover, our graphical statistical analysis indicates that CI binding probably shortens the DNA before long-distance protein–protein interactions allow looping.

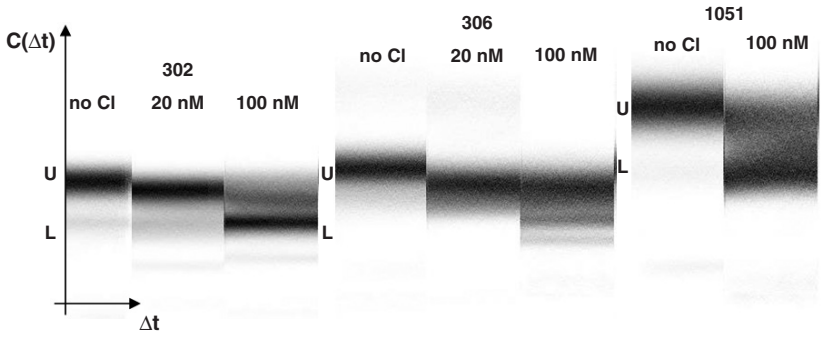

Figure 5. $P(\Delta t, C(\Delta t))$ analysis of TPM measurements using DNA fragments 302, 306 and 1051 in the absence of CI and in the presence of 20 and 100 nM CI. U and L represent the expected levels for the unlooped and the looped DNA conformations respectively.

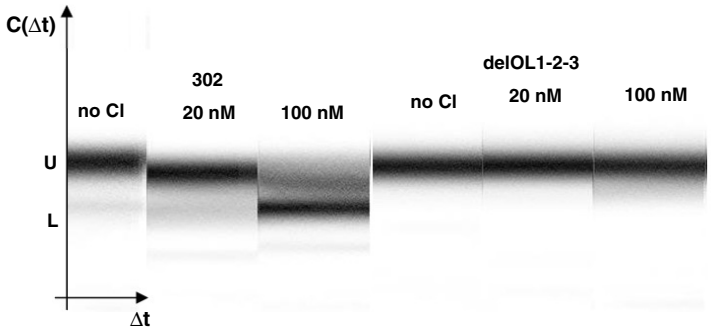

Figure 6. $P(\Delta t, C(\Delta t))$ analysis of TPM measurements performed using the DNA fragments 302 and delOL1-2-3 in the absence of CI and in the presence of 20 and 100 nM CI. U and L represent the expected levels for the unlooped and the looped DNA conformations respectively.

4. Conclusions

In this work we have described an experimental and analytical procedure for performing TPM experiments aimed at studying DNA looping. Protein-induced DNA looping is a frequently observed regulatory mechanism in the physiology of DNA, and has become the focus of numerous biophysical studies, in particular in the field of transcriptional regulation. DNA looping by activators and repressors is often a mechanism of gene regulation [10] and has been also proposed to play an important role in the molecular events that stabilize the switch to the lysogenic state in the life cycle of bacteriophage λ. In this paper we used λ CI protein-induced DNA looping to validate our protocol. We prepared DNA tethers of different lengths and analysed loops of different sizes in order to show that our approach is of general use. Our results indicated that TPM can be applied to a wide range of tether lengths and that the formation of differently sized loops can be monitored. In particular, we were able to show that (1) DNA looping is mediated by CI if both O_L and O_R regions are present, (2) phasing between the O_L and O_R regions may affect the formation of loops approximately 300 bp long and (3) CI-mediated looping occurs even over large distances. Thus, our results support previous evidence of looping in λ obtained by electron microscope analysis [3]. Furthermore, our results support the interpretation that DNA looping is the basis of the long-range cooperativity in gene regulation by the CI repressor, as previously proposed [3, 7]. Our methodology is

a very powerful technique for studying the dynamics of conformational and/or topological changes in single nucleic acid molecules mediated by proteins.

Acknowledgments

We are grateful to Dr Doriano Brogioli for developing the statistical analysis described. This work was partially supported by the Human Frontier Science Foundation (LF), the Italian Ministry for Instruction, Universities and Research, COFIN 2002 and FIRB 2002 (LF and DD) and the Intramural Research Program of the NIH, National Cancer Institute, Centre for Cancer Research.

References

[1] Finzi L and Gelles J 1995 Measurement of lactose-repressor mediated loop formation and breakdown in single DNA molecules *Science* **267** 378
[2] Blumberg S, Gajraj A, Pennington M W and Meiners J 2005 3-D characterization of tethered microspheres by total internal reflection fluorescence microscopy *Biophys. J.* **89** 1272
[3] Revet B, von Wilcken-Bergmann B, Bessert H, Barker A and Muller-Hill B 1999 Four dimers of a lambda repressor bound to two suitably spaced pairs of lambda operators form octamers and DNA loops over large distances *Curr. Biol.* **9** 151
[4] Little J W, Shepley D P and Wert D W 1999 Robustness of a gene regulatory circuit *EMBO J.* **18** 4299
[5] Ptashne M 2005 Regulation of transcription: from lambda to eukaryotes *Trends Biochem. Sci.* **30** 275
[6] Ptashne M 2004 *A Genetic Switch: Phage Lambda Revisited* 3rd edn (Cold Spring Harbor: Cold Spring Harbor Laboratory Press)
[7] Dodd I B, Shearwin K E, Perkins A J, Burr T, Hochschild A and Egan J B 2004 Cooperativity in long-range gene regulation by the λ CI repressor *Genes Dev.* **18** 344
[8] Lewis D E A and Adhya S 2002 In vitro repression of the *gal* promoters by GalR and HU depends on the proper helical phasing of the two operators *J. Biol. Chem.* **277** 2498
[9] Finzi L and Dunlap D D 2003 Single molecule studies of DNA architectural changes induced by regulatory proteins *Methods Enzymol.* **370** 369
[10] Semsey S, Virnik K and Adhya S 2005 A gamut of loops: meandering DNA *Trends Biochem. Sci.* **30** 334